6222 *Inorg. Chem.* **2009**, *48*, 6222–6228
DOI: 10.1021/ic900519p

Inorganic Chemistry
Article

# Second-Order Nonlinear Optical Properties of Polyoxometalate Salts of a Chiral Stilbazolium Derivative

**Jean-Daniel Compain,[†] Pierre Mialane,[†] Anne Dolbecq,*[,†] Jérôme Marrot,[†] Anna Proust,[‡] Keitaro Nakatani,[§] Pei Yu,[∥] and Francis Sécheresse[†]**

[†]*Institut Lavoisier de Versailles, UMR 8180, Université de Versailles Saint-Quentin en Yvelines, 45 Avenue des Etats-Unis, 78035 Versailles cedex, France,* [‡]*Institut Parisien de Chimie Moléculaire, case courrier 42, UMR CNRS 7201, Université Pierre et Marie Curie—Paris 6, 4 Place Jussieu, 75252 Paris cedex 05, France,* [§]*Laboratoire de Photophysique et Photochimie Supramoléculaire et Macromoléculaire, UMR 8531 Institut d'Alembert, Ecole Normale Supérieure de Cachan, PRES Universud, 61 Avenue du Président Wilson, 94235 Cachan, France, and* [∥]*Institut de Chimie Moléculaire et des Matériaux d'Orsay, UMR 8182, Equipe Chimie Inorganique, Univ. Paris-Sud, 91405 Orsay cedex, France*

Received March 17, 2009

The synthesis of nonlinear optical (NLO) active salts with stilbazolium derivatives and polyoxometalate (POM) counterions has been investigated. With known nonchiral stilbazolium derivatives, such as $MOMS^+$, compounds with centrosymmetric structures have been isolated, like for instance the centrosymmetric salt $(MOMS)_4[Mo_8O_{26}]$ (**1**), synthesized under hydrothermal conditions. A new chiral derivative of the known $DAMS^+$ molecules, named here $CHIDAMS^+$, has therefore been synthesized in order to force the crystallization of the hybrid ionic salts in noncentrosymmetric space groups. The $CHIDAMS^+$ cation has been crystallized under two polymorphic $PF_6^-$ salts, $(CHIDAMS)PF_6$ (**2a** and **2b**), and its reactivity with various POMs has been investigated. The ionic salt $(CHIDAMS)_2[Mo_5O_{13}(OEt)_4(NO)\{Na(H_2O)_{0.5}(DMF)_{0.5}\}]$ (**4**) crystallizes in the noncentrosymmetric $P2_1$ group, but the push−pull axis of the $CHIDAMS^+$ cations adopts a quasi-antiparallel alignment. The ionic salt $(CHIDAMS)_3[PW_{12}O_{40}]\cdot 2DMF$ (**5**) associating three $CHIDAMS^+$ cations and a $PW_{12}O_{40}^{3-}$ Keggin anion crystallizes also in the $P2_1$ space group, but the disposition of the cations in the solid state is far more favorable. Diffuse reflectance experiments have evidenced a charge transfer between the organic and inorganic components in **5**, and Kurtz−Perry experiments show that this salt exhibits a second harmonic generation efficiency more than 10 times higher than those of the $PF_6^-$ salts **2a** and **2b**, the hybrid salt **4**, and all of the other NLO active POM molecular materials reported in the literature.

## Introduction

In the field of molecular materials, nonlinear optical (NLO) materials have been attracting continuous interest, because of their potential applications in telecommunications, optical computing, optical data storage, and optical information processing.[1] The molecules exhibiting the largest molecular hyperpolarizability ($\beta$) belong to the stilbazolium family.[2] These molecules possess an electron acceptor linked to an electron donor group through a $\pi$-conjugated bridge. Two examples of stilbazolium derivatives are shown in Figure 1a. The crystallization of $DAMS^+$ molecules with *p*-toluenesulfonate (tosylate) anions has afforded a material known as DAST, with one of the largest powder second harmonic generation (SHG) efficiencies known.[3] However, not all of the molecular materials crystallizing with this chromophore exhibit solid-state NLO properties.[2] Indeed, in order to get an observable bulk nonlinear susceptibility ($\chi^{(2)}$), the molecules must adopt a parallel alignment in the crystal. The required condition to avoid antiparallel alignment is that the material crystallizes in a noncentrosymmetric space group. Many efforts have thus been devoted to the research of counterions which would favor the proper alignment of the organic molecules in the solid state. For instance,

*To whom correspondence should be addressed. E-mail: dolbecq@chimie.uvsq.fr.

(1) See, for example: (a) *Molecular Nonlinear Optics: Materials, Physics and Devices*; Zyss, J., Ed.; Academic Press: New York, 1994.(b) Delaire, J. A.; Nakatani, K. Chem. Rev. 2000, 100, 1817. (c) DiBella, S. Chem. Soc. Rev. 2001, 30, 355. (d) Special Issue on Molecular Photonic Molecules, Materials, Devices: C.R. Acad. Sci. Phys. 2002, 3, 403.

(2) Marder, S. R.; Perry, J. W.; Yakymyshyn, C. P. *Chem. Mater.* **1994**, *6*, 1137.

(3) Marder, S. R.; Perry, J. W.; Schaeffer, W. P. *Science* **1989**, *245*, 626.


Published on Web 05/29/2009

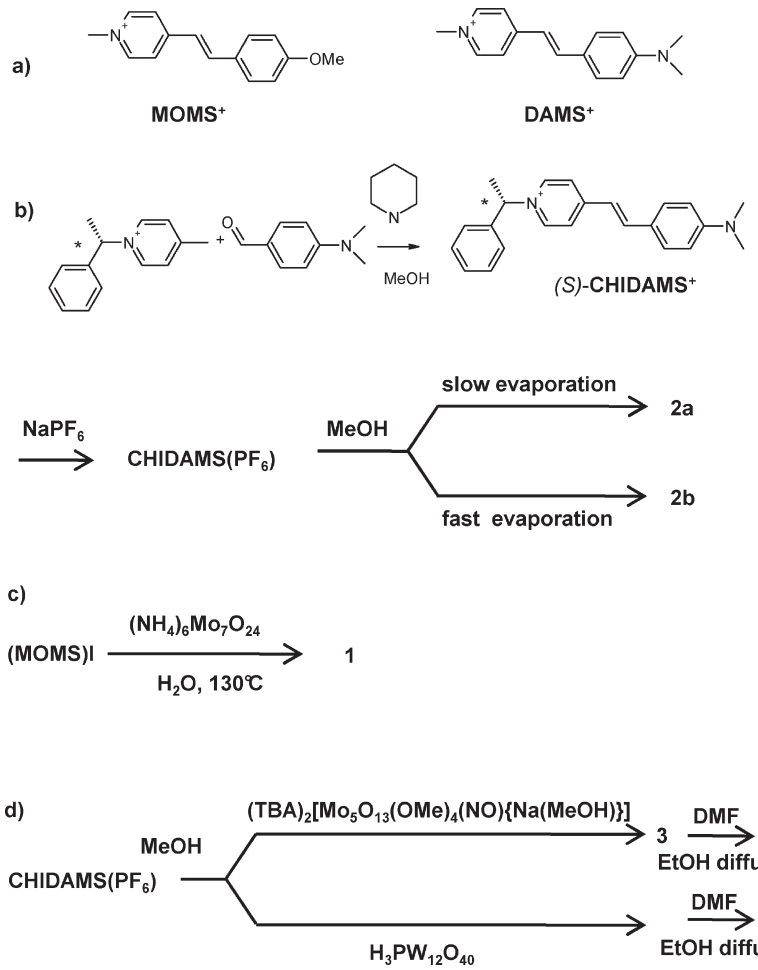


**Figure 1.** (a) Structure of the stilbazolium derivatives and their abbreviations. (b, c, and d) Synthetic pathways to compounds **1**−**5**.

various anions, either molecular or bidimensional, have been crystallized with $DAMS^+$, such as tosylate derivatives (2-naphtalenesulfonate[4] and 2,4,6-trimethylbenzenesulfonate[5]), $[Ni(dmit)_2]^-$ (dmit = 2-thioxo-1,3-dithiole-4,5-dithiolato),[6] tetracyanoquinodimethane,[7] $[M^{III}_2M'^{II}(C_2O_4)_6]^{4-}$ (M = Rh, Fe, Cr; M′ = Mn, Zn) mixed metal oxalates,[8] $MPS_3$ lattices,[9] and $Cu_5I_6$ slabs.[10] Polyoxometalates (POMs) possess a great diversity of shape, composition, and charge and may also exhibit magnetic and catalytic properties.[11] Furthermore, experimental[12] and theoretical[13] studies have shown that POMs themselves can possess molecular hyperpolarizabilities. However, there have only been a few reports of NLO active molecular materials with POM anions, namely, $H_4SiW_{12}O_{40}\cdot 4HMPA\cdot 2H_2O$ (HMPA = hexamethylphosphoramide),[14] $[DAMS][NH_2Me_2]_2HSiFeMo_{11}O_{40}\cdot 3H_2O$,[15] $[(R)\text{-}C_5H_{14}N_2][(MoO_3)_3(SO_4)]\cdot H_2O$,[16] $[H_3O][3\text{-}HPBIM]_2[PW_{12}O_{40}]$ (3-HPBIM = 2-(3-pyridyl)-benzimidazolium),[17] $(H_2bipy)_2[Mo_5{}^{VI}S_2O_{21}]\cdot H_2O$,[18] and $[(S)\text{-}aqnH_2]_2[Mo_8O_{26}]$ (aqn = 3-aminoquinuclidine),[19] probably because of the difficulty in crystallizing materials in noncentrosymmetric space groups. One way to force the growth of molecular salts in chiral space groups is the introduction of a chiral center in the organic molecules. We have thus initiated a project on the crystallization of chiral stilbazolium molecules with, as noninnocent anions, POMs, and we present in this paper the synthesis, structure, and NLO

(4) Ruiz, B.; Yang, Z.; Gramlich, V.; Jazbinsek, M.; Günter, P. *J. Mater. Chem.* **2006**, *16*, 2389.
(5) Yang, Z.; Mutter, L.; Stillhart, M.; Ruiz, B.; Aravazhi, S.; Jazbinsek, M.; Schneider, A.; Gramlich, V.; Günter, P. *Adv. Funct. Mater.* **2007**, *17*, 2018.
(6) Malfant, I.; Andreu, R.; Lacroix, P. G.; Faulmann, C.; Cassoux, P. *Inorg. Chem.* **1998**, *37*, 3361.
(7) Andreu, R.; Malfant, I.; Lacroix, P. G.; Gornitzka, H.; Nakatani, K. *Chem. Mater.* **1999**, *11*, 840.
(8) Criati, E.; Macchi, R.; Roberto, D.; Ugo, R.; Galli, S.; Casati, N.; Macchi, P.; Sironi, A.; Bogani, L.; Caneshi, A.; Gatteschi, D. *J. Am. Chem. Soc.* **2007**, *129*, 9410.
(9) Coradin, T.; Clément, R.; Lacroix, P. G.; Nakatani, K. *Chem. Mater.* **1996**, *8*, 2153.
(10) Cariati, E.; Ugo, R.; Cariati, F.; Roberto, D.; Masciocchi, M.; Galli, S.; Sironi, A. *Adv. Mater.* **2001**, *13*, 1665.
(11) Special edition on polyoxometalates: *Chem. Rev.* **1998**, *98*, 1−390 (Hill, C. L., Ed.).
(12) Murakami, H.; Kozeki, T.; Susuki, Y.; Ono, S.; Ohtake, H.; Sarukura, N.; Ishikawa, E.; Yamase, T. *Appl. Phys. Lett.* **2001**, *79*, 3564.
(13) (a) Guan, W.; Yang, G.-C.; Yan, L.-K.; Su, Z.-M. *Eur. J. Inorg. Chem.* **2006**, 4179. (b) Yan, L.-K.; Jin, M.-S.; Zhuang, J.; Liu, C.-G.; Su, Z.-M.; Sun, C.-C. *J. Phys. Chem. A* **2008**, *112*, 9919.
(14) Niu, J.-Y.; You, X.-Z.; Duan, C.-Y. *Inorg. Chem.* **1996**, *35*, 4211.
(15) Zhang, X.-M.; Shan, B.-Z.; Duan, C.-Y.; You, X.-Z. *Chem. Commun.* **1997**, 1131.
(16) Muller, E. A.; Cannon, R. J.; Sarjeant, A. N.; Ok, K. M.; Halasyamani, P. S.; Norquist, A. J. *Cryst. Growth Des.* **2005**, *5*, 1913.
(17) Xie, Y.-M.; Zhang, Q.-S.; Zhao, Z.-G.; Wu, X.-Y.; Chen, S.-C.; Lu, C.-Z. *Inorg. Chem.* **2008**, *47*, 8086.
(18) Kapakoglou, N. I.; Panagiotis, B. I.; Kazianis, S. E.; Kosmidis, C. E.; Drouza, C.; Manos, M. J.; Sigalas, M. P.; Keramidas, A. D.; Kabanos, T. A. *Inorg. Chem.* **2007**, *46*, 6002.
(19) Veltman, T. R.; Stover, A. K.; Sarjeant, A. N.; Ok, K. M.; Halasyamani, P. S.; Norquist, A. J. *Inorg. Chem.* **2006**, *45*, 5529.

measurements of five crystalline materials with either the $MOMS^+$ cation or a new chiral $DAMS^+$ derivative.

## Experimental Section

**Synthesis.** The synthetic pathways are summarized in Figure 1. All chemicals were of reagent grade and were used as received. (*S*)-1-(1-Phenylethyl)picolinium chloride,[20] $[n\text{-}(C_4H_9)_4N]_2[Mo_5O_{13}(OMe)_4(NO)\{Na(MeOH)\}]\cdot 3MeOH$,[21] $H_3PW_{12}O_{40}\cdot 20H_2O$,[22] and (MOMS)I[9] were synthesized according to literature procedures.

**$(MOMS)_4[Mo_8O_{26}]$ (1).** The hydrothermal synthesis was carried out in a polytetrafluoroethylene-lined stainless steel container under autogenous pressure. The 23 mL vessel was filled to approximately 25% volume capacity ($V_i$ = 6 mL). A mixture of ammonium heptamolybdate (0.120 g, 0.097 mmol) and (MOMS)I (0.080 g, 0.23 mmol) in 5 mL of water was stirred, and the pH was adjusted to 6.0 by the dropwise addition of 2 M sodium hydroxide. The mixture was then heated for 40 h at 130 °C and cooled down to room temperature over a period of 44 h. Small light yellow crystals were collected and washed with water and ethanol (yield 103 mg, 79% based on MOMS). IR (KBr pellets): $\nu$ ($cm^{-1}$) 1641 (m), 1618 (s), 1599 (s), 1571 (m), 1515 (s), 1470 (m), 1421 (w), 1304 (w), 1260 (m), 1172 (s), 1019 (w), 933 (s), 906 (s), 863 (m), 833 (m), 721 (m). Elem anal. calcd for $C_{60}H_{64}Mo_8N_4O_{30}$ (found): C, 34.50 (34.31); H, 3.09 (3.03); N, 2.68 (2.66); Mo, 36.75 (36.74).

**$(CHIDAMS)PF_6$ (2).** To a solution of (*S*)-1-(1-phenylethyl) picolinium chloride (0.57 g, 2.43 mmol) in 7.5 mL of methanol were added 4-dimethylaminobenzaldehyde (0.36 g, 2.42 mmol) and piperidine (250 $\mu$L, 2.52 mmol). The resulting red solution was refluxed overnight and allowed to cool at room temperature before the addition of sodium hexafluorophosphate (0.43 g, 2.5 mmol). The resulting suspension was stirred for 1.5 h at room temperature; then, the dark orange powder of ((*S*)-CHIDAMS) $PF_6$ (**2**) was filtrated under vacuum conditions and rinsed with small portions of ethanol and diethyl ether (yield 0.75 g, 65%). The optical rotation of a solution of **2** (5.2 mg) dissolved in 100 mL of acetone was measured at 365 nm, at 20 °C, affording the value $[\alpha]_D = +2000$. $^1H$ NMR ($(CD_3)_2SO$): $\delta$ 1.99 (d, 3H); 3.02 (s, 6H); 6.00 (q, 1H); 6.77 (d, 2H); 7.15 (d, 1H); 7.46 (m, 5H); 7.58 (d, 2H); 7.90 (d, 1H); 8.04 (d, 2H); 8.88 (d, 2H). IR (KBr pellets): $\nu$ ($cm^{-1}$) 1642 (m), 1589 (vs), 1579 (vs), 1528 (s), 1366 (m), 1329 (m), 1187 (m), 1156 (s), 1122 (m), 841 (vs), 824 (s). Elem anal. calcd for $C_{23}H_{25}F_6N_2P$ (found): C, 57.85 (57.68); H, 5.25 (5.31); N, 5.93 (5.90); F, 21.16 (24.03); P, 6.30 (6.52). The crude product could be recrystallized from hot methanol. Slow evaporation of a solution of 100 mg of **2** in 15 mL of MeOH yielded almost quantitatively dark red needles of **2a**, while evaporation of a more concentrated solution, prepared by dissolving 100 mg of **2** in 2 mL of MeOH, led to another crystalline phase, **2b**, as thin orange parallelepipeds.

**$(CHIDAMS)_2[Mo_5O_{13}(OR)_4(NO)\{Na(H_2O)_x(DMF)_{1-x}\}]$ (3: R = Me, $x$ = 1; 4: R = Et, $x$ = 0.5; DMF = dimethylformamide).** To a solution of $[n\text{-}(C_4H_9)_4N]_2[Mo_5O_{13}(OMe)_4(NO)\{Na(MeOH)\}]\cdot 3MeOH$ (0.100 g, 0.07 mmol) in 5 mL of methanol was added a solution of **2** (0.070 g, 0.15 mmol) in 10 mL of methanol. The resulting suspension was allowed to stir at room temperature for around 45 min; then, the red precipitate of $(C_{23}H_{25}N_2)_2[Mo_5O_{13}(OMe)_4(NO)\{Na(H_2O)\}]$ (**3**) was filtrated under vacuum conditions and washed with methanol and diethyl ether (yield 92 mg, 82% based on Mo). IR (KBr pellets): $\nu$ ($cm^{-1}$) 1665 (w), 1615 (m), 1580 (vs), 1523 (s), 1462 (m), 1435 (m), 1362 (m), 1324 (m), 1184 (m), 1137 (s), 1090 (m), 1040 (m), 920 (s), 896 (s), 878 (sh). Elem anal. calcd for $C_{50}H_{64}Mo_5N_5NaO_{19}$ (found): C, 38.95 (38.66); H, 4.18 (4.29); N, 4.54 (4.44); Mo, 31.11 (30.71); Na, 1.49 (1.32). The crude powder of **3** could be crystallized from dimethylformamide with the slow diffusion of ethanol, affording in poor yield small dark red needles of $(C_{23}H_{25}N_2)_2[Mo_5O_{13}(OEt)_4(NO)\{Na(H_2O)_{0.5}(DMF)_{0.5}\}]$ (**4**) after a couple of days.

**$(CHIDAMS)_3[PW_{12}O_{40}]\cdot 2DMF$ (5).** To a solution of $H_3PW_{12}O_{40}\cdot 20H_2O$ (0.160 g, 0.05 mmol) in 5 mL of methanol was added a solution of **2** (0.070 g, 0.15 mmol) in 10 mL of methanol. The resulting suspension was allowed to stir at room temperature for around 45 min; then, the red precipitate was filtrated under vacuum conditions and washed with methanol and diethyl ether (yield 194 mg, 98% based on W). The crude powder could be recrystallized from dimethylformamide with the slow diffusion of ethanol, affording small parallelepipedic, dark red crystals after several days. IR (KBr pellets): $\nu$ ($cm^{-1}$) 1666 (m), 1640 (m), 1574 (s), 1525 (s), 1468 (m), 1434 (m), 1373 (m), 1327 (m), 1302 (w), 1205 (m), 1187 (m), 1136 (s), 1078 (s), 976 (s), 893 (s), 809 (vs). Elem anal. calcd for $C_{72}H_{82}N_7O_{41}PW_{12}$ (found): C, 22.45 (22.31); H, 2.24 (2.18); N, 2.79 (2.38); P, 0.77 (0.83); W, 54.99 (54.90).

**X-Ray Crystallography.** Intensity data collections were carried out with a Bruker Nonius X8 APEX 2 diffractometer for **1**, **2b**, and **4** and with a Siemens SMART three-circle diffractometer for **2a** and **5**, each equipped with a CCD bidimensional detector using the monochromatized wavelength $\lambda$(Mo K$\alpha$) = 0.71073 Å. The absorption correction was based on multiple and symmetry-equivalent reflections in the data set using the SADABS program[23] on the basis of the method of Blessing.[24] The structures were solved by direct methods and refined by full-matrix least-squares using the SHELX-TL package.[25] In the structure of **1**, one of the phenyl rings of the $MOMS^+$ cation is disordered over two positions. Each position has been refined with half occupancy. Despite many efforts (not less than five data sets have been recorded on five different crystals, isolated under various experimental conditions), it was not possible to obtain an entirely satisfying data set for **5** probably because of twinning problems. We give here the results for the best one. It was not possible to refine anisotropically the oxygen atoms of the anion; the carbon and nitrogen atoms of the organic molecules and some distances and angles for the organic molecules are not satisfactory, even after the application of constraints. For this compound, we have not attempted to place the hydrogen atoms on the organic molecules. Furthermore, the data set for **5** which contains large voids occupied by solvent molecules was corrected with the program SQUEEZE, a part of the PLATON package of crystallographic software used to calculate the solvent disorder area and remove its contribution to the overall intensity data.[26] As **2b** and **4** rapidly lose water at room temperature, the single crystals of these two compounds were glued in Paraton-N oil and the data set collected at 100 K. Crystallographic data are given in Table 1.

**Elemental Analysis.** Mo, W, Na, and P elements were analyzed on an inductively coupled plasma−atomic emission spectrometry 3580 Thermo electron atomic emission spectrometer. C, H, and N analyses were performed on an SCA elemental analyzer. These analyses were performed by the Service Central d'Analyze Elémentaire, CNRS, 69360 Solaize, France.

**Infrared Spectra.** IR spectra were recorded on an IRFT Magna 550 Nicolet spectrophotometer using the pressed KBr pellets technique.

(20) Genisson, Y.; Marazano, C.; Mehmandoust, M.; Gnecco, D.; Das, B. C. *Synlett* **1992**, 431–434.
(21) Proust, A.; Gouzerh, P.; Robert, F. *Inorg. Chem.* **1993**, *32*, 5291–5298.
(22) Souchet, P. *Ions minéraux condensés*; Masson & Cie: Paris, 1969.
(23) Sheldrick, G. M. *SADABS*; University of Göttingen: Göttingen, Germany, 1997.
(24) Blessing, R. *Acta Crystallogr.* **1995**, *A51*, 33.
(25) Sheldrick, G. M. *SHELX-TL*, version 5.03; Siemens Analytical X-ray Instrument Division: Madison, WI, 1994.
(26) van der Sluis, P.; Spek, A. L. *Acta Crystallogr, Sect. A* **1990**, *46*, 194.

**Table 1.** Crystallographic Data for **1**, **2a**, **2b**, **4**, and **5**

| | **1** | **2a** | **2b** | **4** | **5** |
|---|---|---|---|---|---|
| empirical formula | $C_{60}H_{64}Mo_8N_4O_{30}$ | $C_{23}H_{25}F_6N_2P$ | $C_{23}H_{25}F_6N_2P$ | $C_{55.5}H_{74.5}Mo_5N_{5.5}NaO_{19}$ | $C_{72}H_{82}N_7O_{41}PW_{12}$ |
| fw, g | 2088.67 | 474.42 | 474.42 | 1625.40 | 3938.62 |
| cryst syst | triclinic | orthorhombic | monoclinic | monoclinic | monoclinic |
| space group | $P\bar{1}$ | $P2_12_12_1$ | $P2_1$ | $P2_1$ | $P2_1$ |
| $a$/Å | 9.6675(2) | 10.1825(7) | 6.5241(4) | 12.729(1) | 12.657(1) |
| $b$/Å | 10.3217(3) | 11.0652(8) | 7.9380(5) | 15.6876(2) | 30.787(4) |
| $c$/Å | 18.5294(5) | 40.897(3) | 22.121(1) | 16.649(2) | 14.009(2) |
| α/deg | 80.782(2) | 90 | 90 | 90 | 90 |
| $\beta$/deg | 80.830(1) | 90 | 90.980(3) | 99.676(5) | 114.83(3) |
| $\gamma$ /deg | 68.456(1) | 90 | 90 | 90 | 90 |
| $V$/Å$^3$ | 1687.36(8) | 4607.9(6) | 1145.5(1) | 3277.4(6) | 4954.2(10) |
| $Z$ | 1 | 8 | 2 | 2 | 2 |
| $T$/K | 293 | 293 | 100 | 100 | 293 |
| $\rho_{calcd}$/g cm$^{-3}$ | 2.055 | 1.368 | 1.376 | 1.647 | 2.640 |
| $\mu$/mm$^{-1}$ | 1.528 | 0.180 | 0.181 | 1.008 | 13.966 |
| data/params | 10016/524 | 13487/548 | 6574/292 | 10883/781 | 16823/561 |
| $R_{int}$ | 0.0457 | 0.0724 | 0.0341 | 0.0690 | 0.0888 |
| GOF | 1.090 | 0.990 | 1.039 | 1.064 | 1.004 |
| $R$ ($> 2\sigma(I)$) | $R_1 = 0.0274$ | $R_1 = 0.0772$ | $R_1 = 0.0589$ | $R_1 = 0.0532$ | $R_1 = 0.0939$ |
| | $wR_2 = 0.0650$ | $wR_2 = 0.2091$ | $wR_2 = 0.1502$ | $wR_2 = 0.1232$ | $wR_2 = 0.2297$ |

$^a R_1 = \frac{\sum ||F_o| - |F_c||}{\sum |F_c|}$ $^b wR_2 = \sqrt{\frac{\sum w(F_o^2 - F_c^2)^2}{\sum w(F_o^2)^2}}$

Electronic absorption spectra were recorded on a Perkin-Elmer Lambda 19 spectrometer. For diffuse reflectance measurements, an integrating sphere was used and measurements were performed on pressed pellets obtained by dispersing around 1 mg of the sample in 100 mg of KBr.

**NLO Measurements.** The second-order optical nonlinearities were investigated by SHG using the Kurtz−Perry powder technique.[27] The 1064 nm initial wavelength of a Nd:YAG pulsed laser beam was shifted to 1907 nm by stimulated Raman scattering in a high-pressure hydrogen cell, to avoid the reabsorption of the fundamental or the second harmonic beam. The measurements were performed on uncalibrated microcrystalline powders, obtained by grinding, and put between two glass blades. SHG efficiency was evaluated by taking as a reference the SHG signal of urea recorded under similar conditions. The SHG efficiencies are reported in Table 2 and compared to $KH_2PO_4$ (KDP) using the formula: $I$(urea) = 3 × $I$(KDP).[1a]

## Results and Discussions

**Syntheses and Spectroscopy.** In a first approach, we have crystallized known stilbazolium molecules such as MOMS$^+$ (Figure 1a) with isopolyoxomolybdates under hydrothermal conditions. Hydrothermal conditions are indeed a powerful tool for the crystallization of ionic hybrid organic−inorganic materials. For example, noncentrosymmetric compounds with molybdate and amines have been recently reported.[16,28] We have thus successfully isolated several salts. However, all of the ionic salts we were able to isolate as pure crystalline phases crystallize in centrosymmetric space groups. As an example, we will describe below the structure of $(MOMS)_4[Mo_8O_{26}]$ (**1**), which was synthesized by the reaction of ammonium heptamolybdate and MOMS$^+$ at 130 °C (Figure 1c). We have thus attempted to force the crystallization of the hybrid salts in a noncentrosymmetric space group by the incorporation of a chiral center on the DAMS$^+$ cation. This strategy has already been exploited, and the syntheses of chiral diaminodicyanoquinodimethane molecules,[29] chiral polyesters with azobenzene moieties,[30] and the chiral stilbazolium derivatives MPMS$^+$ [7] and HPMS$^+$ [31] have been reported. The chloride salt of the chiral stilbazolium molecule, named here CHIDAMS$^+$, was prepared through the base-catalyzed condensation of (*S*)-1-(1-phenylethyl)picolinium chloride with 4-(dimethylamino)benzaldehyde and then metathesized to (CHIDAMS)$PF_6$ by precipitation with sodium hexafluorophosphate (Figure 1b). The recrystallization of (CHIDAMS)$PF_6$ afforded two polymorphs, **2a** and **2b**, according to the speed of solvent evaporation. The reactivity of this new chiral stilbazolium derivative toward a great number of POMs has thus been explored, both under hydrothermal conditions and at ambient temperature. We were able to isolate two ionic salts, $(CHIDAMS)_2[Mo_5O_{13}(OEt)_4(NO)\{Na(H_2O)_{0.5}(DMF)_{0.5}\}]$ (**4**) and $(CHIDAMS)_3[PW_{12}O_{40}]\cdot 2DMF$ (**5**), by reacting CHIDAMS$^+$ with $[Mo_5O_{13}(OMe)_4(NO)\{Na(MeOH)\}]^{2-}$ and $PW_{12}O_{40}^{3-}$ respectively. Single crystals have been obtained by recrystallization in DMF (Figure 1d). The synthesis of the highly asymmetric $[Mo_5O_{13}(OMe)_4(NO)\{Na(MeOH)\}]^{2-}$ anion was described by Proust et al. in 1993.[21] The crystals of **4** are obtained by the diffusion of EtOH in a DMF solution, which explains the substitution of the bridging methoxo ligands by ethoxo ligands and the partial removal of the coordinated water molecule on the sodium ion by a DMF molecule.

The UV−vis spectra of the CHIDAMS$^+$ salts **4** and **5** dissolved in DMF have been compared with the spectra of the organic and inorganic precursors (Figure SI1, Supporting Information). The strong absorption band of the CHIDAMS$^+$ molecule is observed at 480 nm in the spectra of **4** and **5**, and the almost exact match of the values of the molar extinction coefficients of **4** ($\varepsilon$ = 87 500 L mol$^{-1}$ cm$^{-1}$) and **5** ($\varepsilon$ = 134 200 L mol$^{-1}$ cm$^{-1}$)

(27) (a) Kurtz, S. K.; Perry, T. T. *J. Appl. Phys.* **1968**, *39*, 3798. (b) Dougherty, J. P.; Kurtz, S. K. *J. Appl. Crystallogr.* **1976**, *9*, 145.
(28) Coué, V.; Dessapt, R.; Bujoli-Doeuff, M.; Evain, M.; Jobic, S. *Inorg. Chem.* **2007**, *46*, 2824.
(29) Ravi, M.; Rao, D. N.; Cohen, S.; Agramat, I.; Radhakrishnan, T. P. *J. Mater. Chem.* **1996**, *6*, 1119.
(30) Bahulayan, D.; Sreekumar *J. Mater. Chem.* **1999**, *9*, 1425.
(31) Lacroix, P. G.; Nakatani, K. *Adv. Mater.* **1997**, *9*, 1105.

**Table 2.** SHG Efficiencies

| compounds | SHG efficiency[a] | ref |
|---|---|---|
| $(MOMS)Mo_8O_{26}$ (**1**) | 0 | this work |
| $(CHIDAMS)PF_6$, **2b** polymorph | ~0 | this work |
| $(H_2bipy)_2[Mo_5^{VI}S_2O_{21}]\cdot H_2O$ | 0.12 | 18 |
| $[(S)\text{-}aqnH_2]_2[Mo_8O_{26}]$ | $<0.4^b$ | 19 |
| $(CHIDAMS)PF_6$, **2a** polymorph | 0.6 | this work |
| $H_4SiW_{12}O_{40}\cdot 4HMPA\cdot 2H_2O$ | 0.71 | 14 |
| $[(R)\text{-}C_5H_{14}N_2][(MoO_3)_3(SO_4)]\cdot H_2O$ | $<0.75^b$ | 16 |
| $[DAMS][NH_2Me_2]_2HSiFeMo_{11}O_{40}\cdot 3H_2O$ | 1.2 | 15 |
| $[H_3O][3\text{-}HPBIM]_2[PW_{12}O_{40}]$ | 2 | 17 |
| $(CHIDAMS)_2[Mo_5O_{13}(OEt)_4(NO)\{Na(H_2O)_{0.5}(DMF)_{0.5}\}]$ (**4**) | 3 | this work |
| $(CHIDAMS)_3[PW_{12}O_{40}]\cdot DMF$ (**5**) | 30 | this work |

[a] Compared to KDP. [b] In refs 16 and 19, the NLO activities are compared to $\alpha$-$SiO_2$, which has an efficiency that is 0.15−0.4 smaller than that of KDP.[1a]

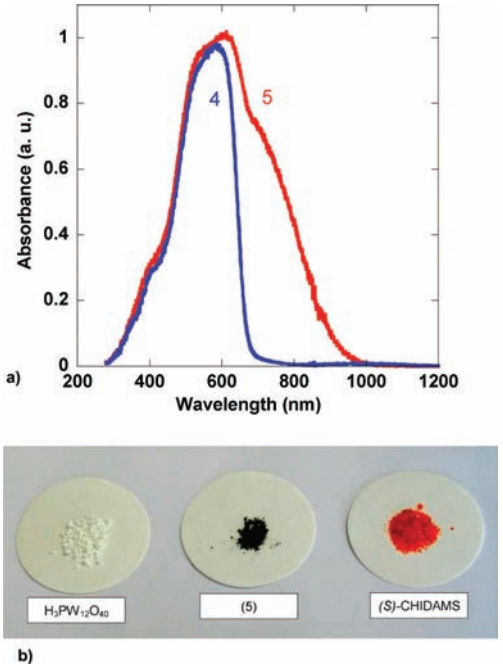


**Figure 2.** (a) Reflectance electronic spectra of **4** and **5**. (b) Comparison of the color of the crystals of **5** with the color of the organic and inorganic precursors.

with the sums of the organic and inorganic components confirm (i) the stoichiometry of the ionic salts and (ii) that in solution $CHIDAMS^+$ cations and POMs do not interact. On the contrary, the reflectance electronic spectrum of **5** (Figure 2a) is different from the superposition of the spectra of $CHIDAMS^+$ and $PW_{12}O_{40}^{3-}$, as in **5** a low-energy tail of the $CHIDAMS^+$ band at ca. 680 nm is observed, which indicates a charge transfer between the organic cations (acting as electron donors) and the POMs (the electron acceptors). Such a charge transfer between organic molecules and Keggin anions has already been reported.[14,17,32,33] No noticeable effect was observed in the diffuse reflectance spectrum of **4** (Figure 2a), probably because of the non-reducibility of the $[Mo_5O_{13}(OMe)_4(NO)\{Na(MeOH)\}]^{2-}$ POM.[19] Indeed, it has been shown that the charge transfer

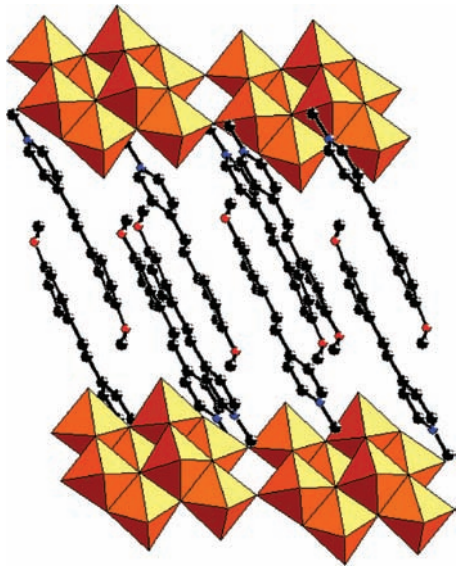

**Figure 3.** View of the structure of **1**, showing the 1D octamolybdate chains running along the *a* axis and the $MOMS^+$ organic molecules between. Orange octahedra, $MoO_6$; black spheres, C; red spheres, O; blue spheres, N; hydrogen atoms have been omitted for clarity.

character of crystalline materials with POMs is correlated to the reduction potentials of the POM acceptors.[34] The dark red, almost black color of the crystals of **5** (Figure 2b), compared to the lighter red color, essentially due to the organic molecule, of the crystals of **4** confirms also the charge transfer in **5** and its absence in **4**. The color of the crystals of **5** fades immediately after dissolution in DMF, in agreement with the dissociation of both components and the cancellation of the charge transfer.

**Structures and NLO Activities.** $(MOMS)_4[Mo_8O_{26}]$ (**1**) crystallizes in the centrosymmetric space group $P\bar{1}$. Its structure consists of $MOMS^+$ cations and infinite anionic $1/_\infty[Mo_8O_{26}]^{4-}$ chains running along the *a* axis, obtained from the condensation of $\gamma$-$\{Mo_8O_{28}\}$ units (Figure 3). A ball-and-stick representation of the octamolybdate chain is given in Figure SI2 (Supporting Information). Three kinds of $1/_\infty[Mo_8O_{26}]^{4-}$ chains have been reported in the literature according to the connecting modes between the subunits.[26] In **1**, the octamolybdate subunits share two corners in a similar way to that observed, for example, in $(Me\text{-}NC_5H_5)_4[Mo_8O_{26}]$.[35] Due to the presence of an

(32) Prosser-McCartha, C. M.; Kadkhodayan, M.; Williamson, M. M.; Bouchard, D. A.; Hill, C. L. *J. Chem. Soc., Chem. Commun.* **1986**, 1747.
(33) Gamelas, J. A. F.; Santos, F. M.; Felix, V.; Cavaleiro, A. M. V.; de Matos Gomes, E.; Belsley, M.; Drew, M. G. B. *Dalton Trans.* **2006**, 1197.
(34) Le Maguers, P.; Hubig, S. M.; Lindeman, S. V.; Veya, P.; Kochi, J. K. *J. Am. Chem. Soc.* **2000**, 10073.
(35) Modec, B.; Brenčič, J. V.; Zubieta, J. *Inorg. Chem. Commun.* **2003**, *6*, 506.

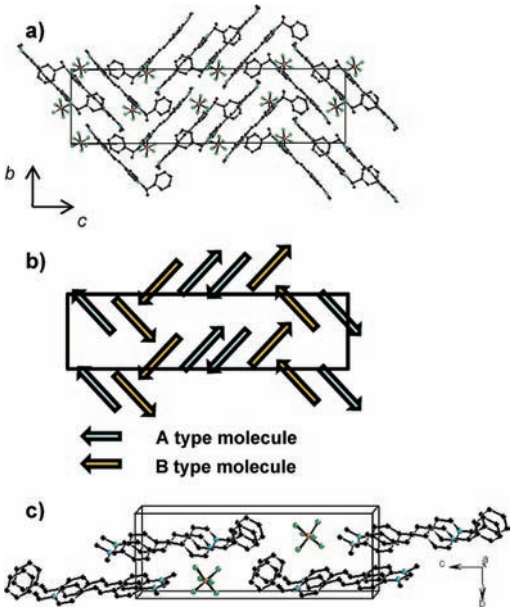


**Figure 4.** (a) View of the unit cell of **2a**. (b) Schematic view of the disposition of A and B types of molecules in the unit cell of **2a**. (c) View of the unit cell of **2b**. Black spheres, C; blue spheres, N; green spheres, F; orange spheres, P; hydrogen atoms have been omitted for clarity.

inversion center, $MOMS^+$ cations are arranged in an exact antiparallel way. As expected, chirality has imposed the crystallization of the two polymorphs **2a** and **2b** in the noncentrosymmetric space groups $P2_12_12_1$ and $P2_1$, respectively. However, the molecular packing is not optimal for second-order NLO effects. Indeed, in **2a**, there are two organic molecules in the asymmetric unit, labeled A and B, which associate into a head-to-tail dimer (Figures 4a,b and Figure SI3a, Supporting Information) favored by $\pi$-orbital overlap. In **2b**, the molecules do not form dimers but alternate with $PF_6^-$ anions in planes perpendicular to the *b* axis; however, in these planes, they align in an antiparallel fashion (Figure 4c and Figure SI4, Supporting Information). In **4**, the POM unit is the $[Mo_5O_{13}(OEt)_4(NO)\{Na(H_2O)_{0.5}(DMF)_{0.5}\}]^{2-}$ anion (Figure 5a), which can be described as a functionalized lacunary Lindquist-type POM.[19] In this anion, a $\{Mo^{II}\text{-}NO\}^{3+}$ group is linked to four $Mo^{VI}$ centers via ethoxo ligands. The lacuna is occupied by a sodium cation which is bound to four terminal oxygen atoms of the POM and to a water molecule disordered with a DMF molecule. In the molecular solid **4**, the POM is surrounded by eight organic ligands which interact with the oxygen atoms of the $\{NO\}^+$ group and the terminal and bridging oxygen atoms of the POM via numerous C−H···O bonds (Figure SI5, Table SI1, Supporting Information). Unfortunately, like in the structures of **2a**, the organic molecules associate into head-to-tail dimers (Figure 5b and Figure SI3b, Supporting Information). The organic cations appear slightly more distorted and closer within a dimer in **4** than in **2a** (Figure SI3b). Finally, in **5**, because of the −3 charge of the POM, there are three independent organic molecules for one POM in the asymmetric unit, labeled A, B, and C. This prevents the formation of dimeric entities (Figure 6a). The charge transfer observed in the solid state for **5** (see above) is canceled in solution, suggesting that the distance between the organic and

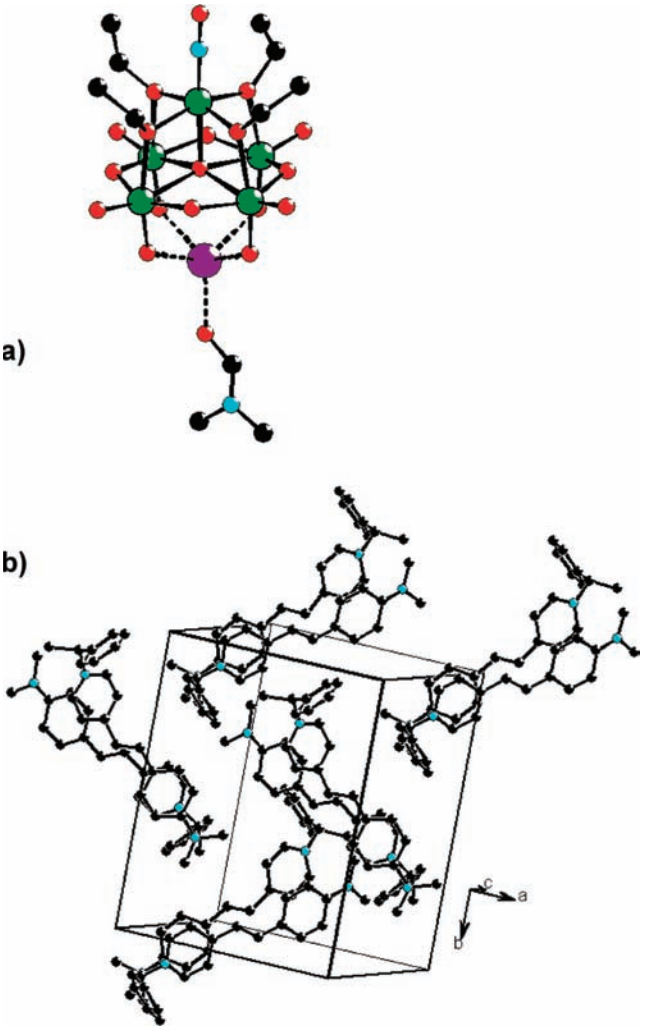


**Figure 5.** (a) Ball-and-stick representation of the $[Mo_5O_{13}(OEt)_4(NO)\{Na(H_2O)_{0.5}(DMF)_{0.5}\}]^{2-}$ POM in **4**. The DMF molecule bound to the sodium ion is disordered with a water molecule. (b) View of the disposition of the organic molecules in **4**. black spheres, C; red spheres, O; blue spheres, N; purple sphere, Na; hydrogen atoms have been omitted for clarity.

inorganic counterparts must play a role. Indeed, short nonbonded C···O distances between the carbon atoms of the organic donor and the oxygen atoms of the anionic POM can be identified (Figure SI6, Table SI2, Supporting Information). The positively charged part of the organic molecule is the closest and acts as a cationic anchor, in a similar manner to what was observed for charge transfer salts with anthracene derivatives and polyoxomolybdate anions.[32] Note also that the B molecules in which $\pi$-donor planes face the oxygen planes of the POM seem to interact better than the other two (Figure SI6). However, as it has not been possible to locate the hydrogen atoms (see Experimental Section), geometrical details on the C−H···O hydrogen bond interactions cannot be given.

The NLO efficiencies of **1**, **2a**, **2b**, **4**, and **5** are reported in Table 2 and compared with compounds of the literature containing POMs as counterions. As expected, no NLO activity is observed for the centrosymetric salt **1**. Furthermore the noncentrosymmetric compounds **2a**, **2b**, and **4**, in which the stibazolium cations adopt a

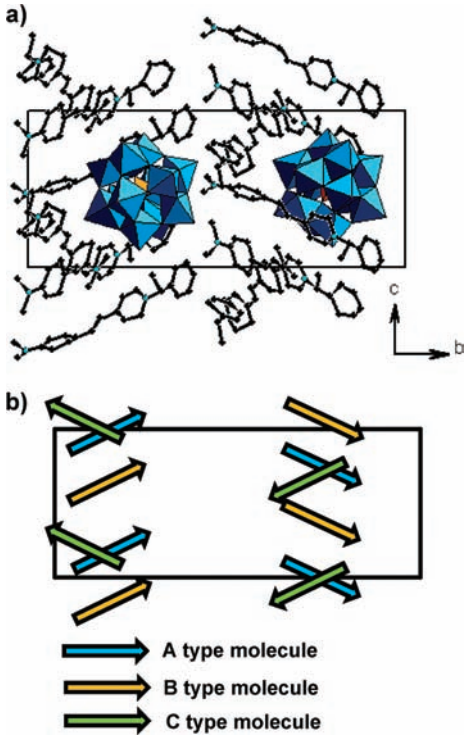


**Figure 6.** (a) View of the unit cell of **5**. (b) Schematic view of the arrangement of the CHIDAMS$^+$ cations: blue octahedra, $WO_6$; orange tetrahedra, $PO_4$; black spheres, C; blue spheres, N.

quasi-antiparrallel arrangement, exhibit only weak optical activity. On the contrary, in **5**, unlike the other structures with the CHIDAMS$^+$ cations, there is no cancellation of the dipole moments of the push−pull organic cations (Figure 6b). In agreement with the solid-state structure, **5** shows very good activity, more than 10 times higher than those of the other reported salts with POM anions.

From this work it can be concluded that the prediction of crystal packing from the molecular structures is not obvious. Some concepts used to quantify chirality have been described in the literature to rationalize the relationship between the chirality of the chromophores, the noncentrosymmetry of the crystal, and physical properties, such as NLO activity,[36] but are difficult to apply here.

## Conclusions

In order to force the crystallization of hybrid organic−inorganic salts in a noncentrosymmetric space group, a condition for the observation of bulk second-order NLO properties, a new chiral stilbazolium cation has been synthesized and crystallized with POMs. The charge-transfer salt with $PW_{12}O_{40}^{3-}$ counterions exhibits the largest SHG activity (30 times that of KDP) among the reported molecular materials with POMs. Further experimental work is in progress in order to crystallize this promising DAMS$^+$ derivative with other POMs, which could optimize the crystal packing and orient the dipolar cations as parallel as possible. Furthermore, the synthesis of other chiral cations with bulky phenyl groups on both sides, which could prevent their tendency to form head-to-tail dimers, is currently under investigation.

**Supporting Information Available:** X-ray crystallographic CIF data in PDF format for **1**, **2a** and **2b**, **4**, and **5** and figures of UV−vis spectra and ball-and-stick representations. This material is free of charge via the Internet at http://pubs.acs.org.

(36) (a) Alvarez, S.; Alemany, P.; Avnir, D. *Chem. Soc. Rev.* **2005**, *34*, 313. (b) Rivera, J. M.; Reyes, H.; Cortés, A.; Santillan, R.; Lacroix, P. G.; Lepetit, C.; Nakatani, K.; Farfáne, N. *Chem. Mater.* **2006**, *18*, 1174.